

Synthesis and properties of push-pull imidazole derivatives with application as photoredox catalysts

Zuzana Hloušková and Filip Bureš*

*Institute of Organic Chemistry and Technology, Faculty of Chemical Technology, University of Pardubice,
Studentská 573, Pardubice, CZ-532 10, Czech Republic*

Email: filip.bures@upce.cz

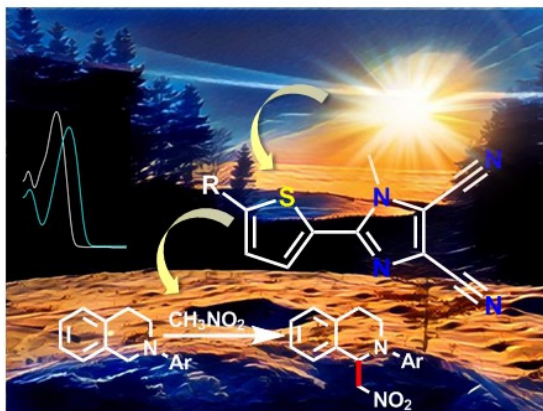
Received 02-24-2017

Accepted 04-16-2017

Published on line 06-11-2017

Abstract

Two new push-pull molecules with imidazole-4,5-dicarbonitrile acceptor, thiophene and 2-methoxythiophene donors with potential use in photoredox catalysis were designed and prepared. The synthesis started from commercially available imidazole-4,5-dicarbonitrile and its bromination and *N*-methylation. Subsequent Suzuki-Miyaura cross-coupling with (5-methoxy)thiophene-derived boronic acids afforded target push-pull derivatives. Beside common analytical methods, the molecular structure of 5-methoxythiophen-2-yl derivative has also been verified by X-ray analysis. DSC analyses showed remarkable thermal stabilities of both target derivatives with T_m and T_D values above 150 and 270 °C, respectively. Fundamental properties and extent of the intramolecular charge-transfer were further studied by UV-VIS absorption spectra and DFT calculations. Fundamental photoredox properties of target imidazole derivatives were elucidated. Both push-pull molecules were preliminary tested as photoredox catalysts in cross-dehydrogenative coupling reaction between tetrahydroisoquinoline and nitromethane and the results were compared with those obtained by pyrazine-2,3-dicarbonitrile-derived catalyst.



Keywords: Imidazole-4,5-dicarbonitrile, push-pull, photoredox catalysis, cross-dehydrogenative coupling

Introduction

Recently, photoredox catalysis, revived as a unique tool in synthetic organic chemistry.¹⁻⁶ Diverse chemical transformations promoted by irradiation with visible light (VL) have been established. In general, VL photoredox reactions can proceed under mild conditions and are considered as environmentally friendly.⁷⁻¹⁰ Historically, photoredox catalysis focused mostly on transition metal complexes¹¹ and especially ruthenium and iridium polypyridyl complexes have been used and are the main representative photoredox catalysts.¹²⁻¹⁷ However, organic dyes such as xanthene dyes fluorescein, eosin Y, eosin B, and rose bengal, represent another significant class of photocatalysts.¹⁸⁻²¹ These compounds are metal-free and significantly less expensive but their further property tuning is very limited. Hence, synthetic small organic molecules with photoredox properties are currently very burgeoning area.¹ As a photoredox catalyst should primarily absorb light in the UV-Vis part of the spectra, π -conjugated molecules equipped with an electron donor (D) and electron acceptor (A), so called push-pull or D- π -A systems, are very promising candidates. In these molecules, intramolecular charge-transfer (ICT) from the donor to the acceptor takes place and a new low-energy molecular orbital is formed. Photoexcitation of the electron from the HOMO to the LUMO in D- π -A molecules is facile and may be accomplished by visible light.^{22,23}

In 2011, we designed and synthesized new X-shaped push-pull chromophores based on 4,5-disubstituted pyrazine-2,3-dicarbonitrile (dicyanopyrazine, DCP) and applied them as tunable chromophores for nonlinear optics (NLO).²⁴ Later on and upon structural tuning, a new DCP derivative **1** substituted with two 5-methoxythienyl donors was developed (Figure 1).²⁵ Derivative **1** is a very efficient photoredox catalyst in various cross-dehydrogenative coupling (CDC) reactions²⁶ as well as in oxidation, oxidative hydroxylation, and reductive dehalogenation.²⁵ Further catalytic performance was demonstrated in chemodivergent radical cascade reactions between *N*-tetrahydroisoquinolines and *N*-itaconimides,²⁷ pH-controlled photooxygenation of indoles,²⁸ and enantioselective oxidative C(*sp*³)-H olefinations.²⁹ In this work, we focus on synthesis of Y-shaped push-pull analogues **2** and **3** based on five-membered acceptor unit – imidazole-4,5-dicarbonitrile (dicyanoimidazole, DCI) and further evaluation of their optoelectronic properties and photoredox catalytic activities. The DCI unit proved to be readily available heterocyclic acceptor for push-pull molecules,³⁰⁻³⁶ however, none of them has been investigated as potential photoredox catalyst. In principal, the structural tuning of the original DCP derivative **1** can be achieved by replacing the acceptor unit (DCP→DCI) and also by variation of the peripheral R-substituent (H or OMe).

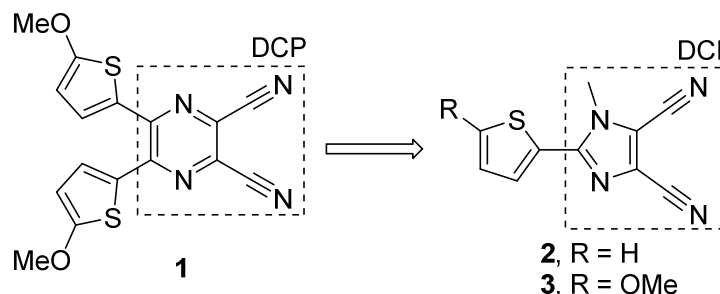
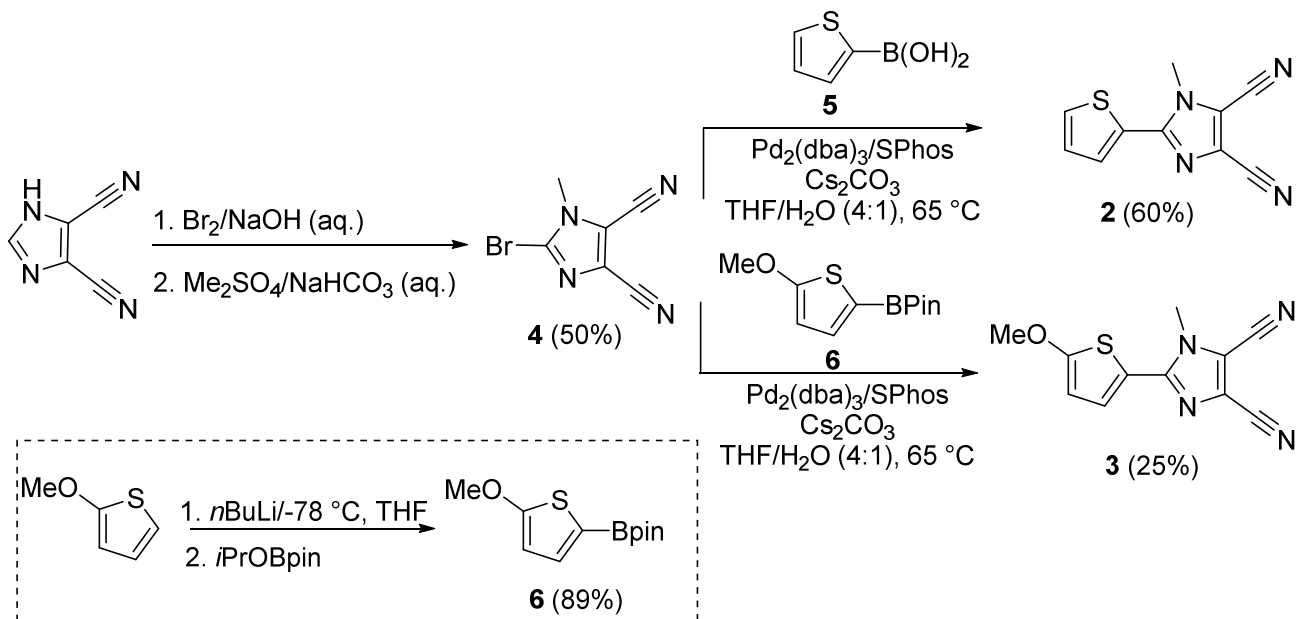


Figure 1. Comparison of DCP and DCI X- and Y-shaped push-pull molecules **1** and **2-3**.

Results and Discussion



Scheme 1. Synthesis of bromo imidazole **4**, pinacol boronate **6** (inset), and target push-pull chromophores **2** and **3**.

Synthesis. The synthesis of target push-pull molecules **2** and **3** started from commercially available imidazole-4,5-dicarbonitrile (Scheme 1). This derivative underwent smooth bromination at the C2 position and subsequent N -methylation preventing imidazole tautomerism.^{32,37,38} As the starting imidazole-4,5-dicarbonitrile is a fairly strong acid, both reactions were easily carried out in alkaline media (aqueous NaOH or NaHCO_3); isolation and purification of **4** involved only precipitation and crystallization. Bromo precursor **4** is well-known to undergo Suzuki-Miyaura cross-coupling, whereas Sonogashira reaction is complicated by a subsequent polymerization.³⁰⁻³⁶ Hence, we introduced the (5-methoxy)thienyl donors via the reaction with commercially available thiophen-2-ylboronic acid **5** and 5-methoxythiophen-2-ylboronic acid pinacol ester **6**. The latter was prepared from 2-methoxythiophene and its lithiation and reaction with 2-isopropoxy-4,4,5,5-tetramethyl-1,3,2-dioxaborolane ($i\text{PrOBpin}$) with 89% yield. Final Suzuki-Miyaura cross-coupling reactions of **4** with **5** and **6** afforded two new DCI push-pull molecules **2** and **3** with 60 and 25% yields, respectively. The Suzuki-Miyaura reactions were carried out under optimized conditions involving $[\text{Pd}_2(\text{dba})_3]$ precatalyst, SPhos ligand, CsCO_3 as a base, and THF/ H_2O (4:1) reaction media.²⁵ This reaction afforded **3** with diminished yield of 25% which was most likely caused by relatively low stability and possible catalytic system contamination by thiophene derivative **6**.^{25,39}

X-ray analysis. Crystals of target molecule **3** suitable for single crystal X-ray analysis were prepared by a slow diffusion of hexane into its CH_2Cl_2 solution. The X-ray representation (Figure 2) confirms the proposed molecular structure. In the solid state, the thiophene sulfur is *anti*-arranged to the methyl group of the DCI acceptor moiety, which allows a very planar arrangement of the entire molecule; the torsion angle between imidazole and thiophene rings is 0.2° (S1-C4-C5-N2). The C-C bond distances within the thiophene ring were found 1.36 (C1-C2), 1.41 (C2-C3), and 1.39 Å (C3-C4). This alternation can be ascribed to the ICT from the methoxy donor to the DCI acceptor. The quinoid character of the central thiophene ring can be determined by the Bird index I_5 .⁴⁰⁻⁴³ Whereas in unsubstituted thiophene, the Bird index is 66, in **3** equals to 63. This implies

less aromatic and higher quinoid character of the thiophene rings in **3**. However, thiophene can be polarized even further by connecting amino donor and indan-1,3-dione acceptor as we have recently demonstrated for T-shaped push-pull molecules ($I_5 = 58$).⁴⁴ The supramolecular arrangement of **3** reveals head to tail chromophore arrangement and 2D-layered array structures with π - π stacking typical for dipolar D- π -A molecules.

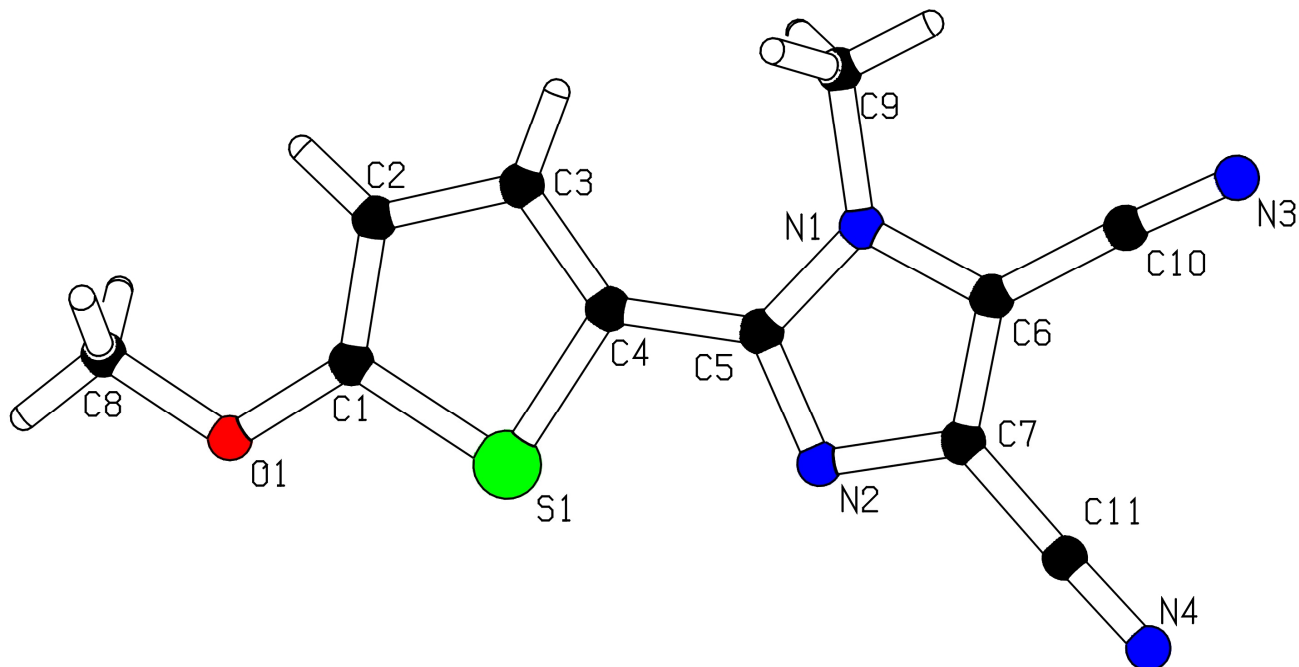


Figure 2. X-ray molecular representation of compound **3**.

Thermal stability. Thermal behavior of DCP and DCI derivatives **1** and **2/3** was studied by differential scanning calorimetry (DSC). Figure 3 shows DSC curves of all three derivatives, Table 1 lists the temperatures of melting and decomposition T_m and T_D , respectively. The measured melting temperatures (endothermic processes, peaks oriented down) were within the range of 149 to 178 °C, while decompositions (exothermic processes, peaks oriented up) of **1** and **3** were measured at 256 and 277 °C, respectively. In contrast, compound **2** resisted decomposition after melting but increasing temperature led to its gradual evaporation from the crucible. A solid-solid transition between α' and α crystalline forms was observed for compound **2** at 134 °C, probably due to its amorphous crystalline character. Within DCI molecules **2** and **3**, the melting point slightly increased upon attaching the methoxy group. In comparison to DCP derivative **1**, both DCI derivatives significantly resisted thermal decomposition up to 277 °C (**3**) or boiling point at 320 °C (**2**).

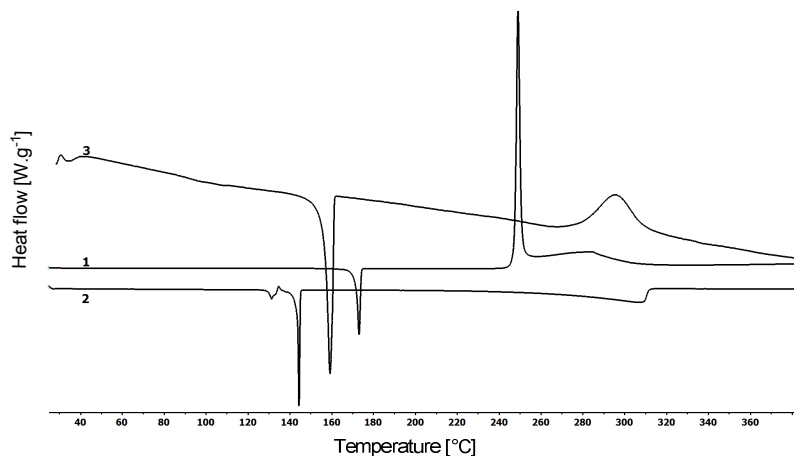


Figure 3. DSC thermograms of studied compounds determined with a scanning rate of 3 °C/min under N₂.

Table 1. Thermal and optical properties of compounds **1-3**

Comp.	T_m [°C]	T_D [°C]	λ_{\max}^A [nm/eV] ^a	ϵ [mol ⁻¹ dm ³ cm ⁻¹] ^a	λ_{\max}^F [nm/eV] ^a	q^F ^b	Stokes shift [cm ⁻¹ / eV] ^a	$E_{0,0}$ [eV] ^c
1	178	256	448/2.77	19 000	552/2.25	0.02	4200/0.52	2.48
2	149	-	296/4.19	14 600	349/3.55	0.25	5130/0.64	3.84
3	156	277	323/3.84	12 900	390/3.18	0.16	5320/0.66	3.48

^a Measured in CH₂Cl₂. ^b Quinine sulphate in 0.5 M aqueous H₂SO₄ ($\lambda_{\max}^F = 445$ nm, $q^F = 0.546$) was used fluorescence standard. ^c Excited state energy; calculated as the midpoint between the absorption and emission maxima.¹

Optical properties. Linear optical properties of push-pull chromophores **2** and **3** were studied by electronic absorption and emission spectroscopy. The absorption spectra along with **1** are shown in Figure 4. All fundamental data such as the longest-wavelength absorption/emission maxima ($\lambda_{\max}^{A/F}$), molar absorption coefficient (ϵ), fluorescence quantum yield (q^F), Stokes shifts, and excited state energies ($E_{0,0}$) are summarized in Table 1. Whereas the UV-Vis absorption spectrum of X-shaped DCP derivative **1** showed two particularly developed CT-bands, DCI imidazoles **2** and **3** showed single bands with the longest-wavelength absorption maxima appearing at 296 and 323 nm. With respect to DCP **1** (λ_{\max} 448 nm), these maxima are hypsochromically shifted by more than 100 nm as a result of lower electron-withdrawing ability of the DCI acceptor unit as well as presence of one vs. two electron-donating (5-methoxy)thienyl moieties.^{22,31} The molar absorption coefficients of imidazole derivatives **2** and **3** are slightly lower as well. However, the absorption maxima of **2** (λ_{\max} 296 nm) can easily be red-shifted by attaching methoxy group as in **3** (λ_{\max} 323 nm). The emission spectra of all three molecules feature one single band appearing between 349 and 552 nm. In contrast to the diminished fluorescence quantum yield of DCP derivative **1** (q^F 0.02), the quantum yields of **2** and **3** are significantly higher (q^F 0.25 and 0.16). These derivatives also possess similar Stokes shifts of about 0.65 eV, which is slightly higher than for **1** (0.52 eV, 4.200 cm⁻¹). Considering (5-methoxy)thienyl ring as a “rotating” substituent, larger Stokes shift (>5.000 cm⁻¹) implies higher geometry reorganization of **2** and **3** upon photoexcitation.⁴⁴ The excited state energies ($E_{0,0}$) referring to the transition between the lowest

vibrational states of the first excited and ground levels S_1 and S_0 were further derived from the absorption and fluorescence spectra (Table 1). These data fall within the range of known values for cyanoarenes (2.90-4.01 eV);¹ however, the calculated $E_{0,0}$ values of DCI derivatives **2** and **3** are ≥ 1 eV higher than that of DCP derivative **1**.

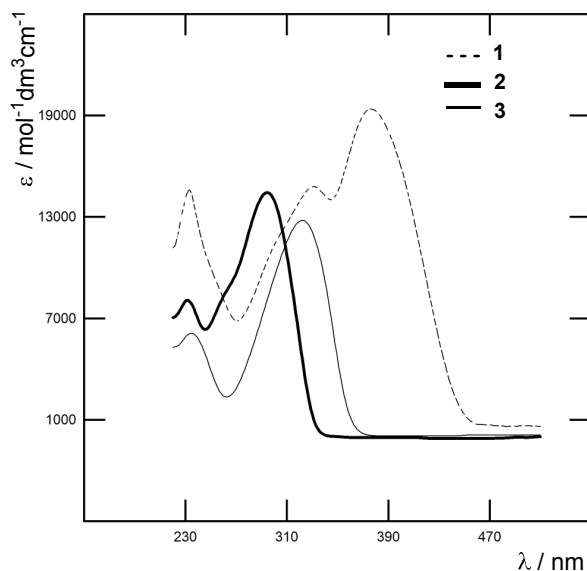


Figure 4. UV-Vis absorption spectra of **1-3** in CH_2Cl_2 ($c = 2 \times 10^{-5}$ M).

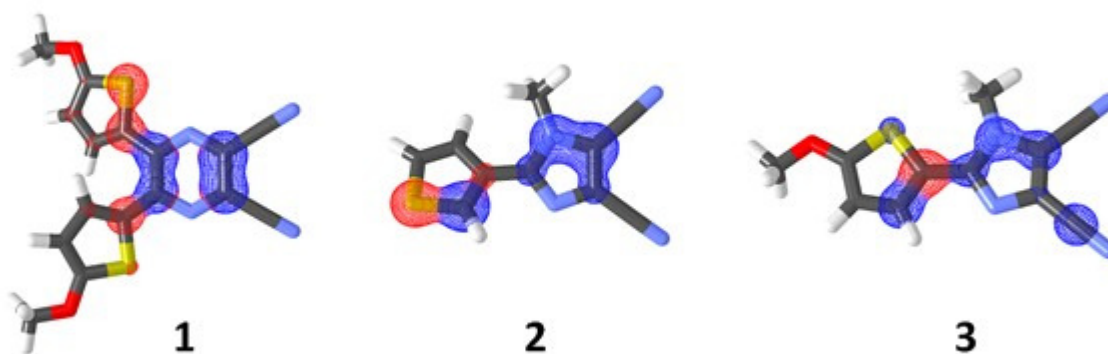
DFT calculations. In contrast to DCP derivative **1**,²⁵ ground state electrochemical properties (especially the first oxidation and reduction potentials) of DCI molecules **2** and **3** were out of the potential window of the employed electrochemical methods (cyclic voltammetry, rotating disc voltammetry or polarography). Hence, these fundamental properties were gained by DFT calculations. The calculations were carried out at the DFT level using Gaussian W09 package.⁴⁶ The geometries were optimized by DFT B3LYP/6-311++G(2df,p) method; energies of the HOMO/LUMO and their differences were calculated on the DFT B3LYP/6-311++G(2df,p) level. All calculated data are summarized in Table 2.

For each particular molecule **1-3**, all possible rotamers with the (5-methoxy)thienyl moieties arranged out/in or *anti/syn* with respect to the pyrazine and *N*-methylimidazole parent scaffold were considered. Figure 5 shows the optimized geometries with the lowest total energies and the HOMO/LUMO localizations. Whereas **1** showed both 5-methoxythienyl moieties oriented outwards, DCI derivatives **2** and **3** possess thiophene sulfur atoms oriented *anti* and *syn* with respect to the imidazole *N*-methyl substituent. Although the rotamer **3** (Figure 5) is opposite to that observed by X-ray analysis (Figure 2), both possess very similar calculated values of the HOMO/LUMO energies. The HOMO and LUMO in DCP derivative **1** are localized on the 5-methoxythiophene donor and DCP acceptor moieties and are well separated as a result of a strong ICT. In DCI derivatives **2** and **3** the LUMO is predominantly localized on the DCI acceptor and partially spread over the appended thiophene ring and the charge separation is thus lower. The HOMO and LUMO energies calculated in DMF were recalculated to the first oxidation and reduction potentials E_{ox} and E_{red} .⁴⁷ These values were further used to estimate the excited state oxidation and reduction potentials E_{ox}^* and E_{red}^* .¹ As can be seen, the DCI derivatives are less easy to oxidize/reduce and possess larger HOMO-LUMO gaps ΔE than DCP derivative **1**. Likewise, the excited state oxidation and reduction potentials are shifted to more negative and positive values, respectively.

Table 2. DFT calculated properties of push-pull chromophores **1-3**

Comp.	Ground state					Excited state		
	E_{HOMO} [eV] ^a	E_{LUMO} [eV] ^a	ΔE [eV] ^a	E_{ox} [eV] ^b	E_{red} [eV] ^b	$E_{0,0}$ [eV] ^c	E_{ox}^* [eV] ^d	E_{red}^* [eV] ^d
1	-5.90	-2.96	2.94	1.55	-1.39	2.48	-0.93	1.09
2	-6.73	-2.26	4.47	2.36	-2.09 ^e	3.84	-1.48	1.75
3	-6.05	-2.22	3.83	1.70	-2.13	3.48	-1.78	1.35

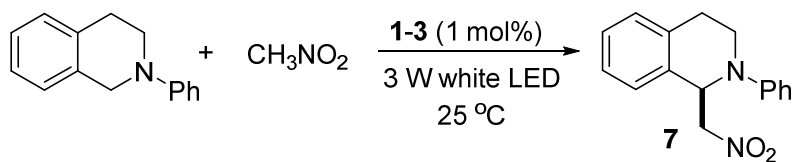
^a Calculated at the DFT B3LYP/6-311++G(2df,p) level (scrfl = solvent = DMF). ^b Re-calculated from the DFT-derived $E_{\text{HOMO/LUMO}}$ according to the equation: $E_{\text{red/ox}} = -E_{\text{HOMO/LUMO}} - 4.35$ (Ref.⁴⁷). ^c Taken from Table 1. ^d Calculated as follows: $E_{\text{ox}}^* = E_{\text{ox}} - E_{0,0}$ and $E_{\text{red}}^* = E_{\text{red}} + E_{0,0}$ (Ref.¹). ^e The only one electrochemically obtained value of $E_{1/2(\text{red})} = -1.94$ V vs. SCE.

**Figure 5.** Optimized geometries and HOMO (red) and LUMO (blue) localizations in push-pull molecules **1-3**.

Catalytic activity. Fundamental photoredox properties of push-pull DCI derivatives **2-3** and DPZ derivative **1** were examined in model cross-dehydrogenative coupling (CDC) between *N*-phenyltetrahydroisoquinoline and nitromethane (Table 3). The reactions were carried out with 1 mol% catalysis of **1-3** by irradiating the reaction mixture with 3W white LED under air at 25 °C. Nitromethane was used as nucleophile as well as solvent. The catalytic performance of DCP and DCI derivatives differ substantially. Whereas the reaction catalyzed with **1** afforded **7** with the yield of 69% within 2 h, the reaction times of DCI catalysts **2** and **3** were considerably longer. Even after 47 h, the attained yields did not exceeded 50%. These low catalytic outcomes reflect the aforementioned properties of both DCI catalysts. Namely, we can deduce the following structure-property relationships:

- Absorption maxima of both DCI derivatives **2** (λ_{max} 296 nm) and **3** (λ_{max} 323 nm) are far from the high energy emission band of a white LED (~430 nm).
- The absorption maxima of DCP derivative **1** (λ_{max} 448 nm) fits the white LED emission band almost perfectly.
- These differences in fundamental optical properties are reflected in the lowest catalytic performance of DCI derivatives **2** and **3**.
- However, catalysts **3** with an additional methoxy substituent, and thus red-shifted CT-band, showed better catalytic performance than unsubstituted **2**.

Table 3. CDC reaction



Comp.	<i>t</i> [h]	Yield [%]
1	2	69
2	47	26
3	47	42

Conclusions

Based on the molecular structure of successful DCP photoredox catalyst **1**, we have designed new push-pull molecules **2** and **3** with a five-membered DCI acceptor unit. The electron-donating part represents (5-methoxy)thiophene. These molecules were prepared by Suzuki-Miyaura cross-coupling reactions of 2-bromo-1-methyl-1*H*-imidazole-4,5-dicarbonitrile with appropriate boronic acids. Beside standard analytical methods (NMR, MS, IR), the molecular structure of **3** was also supported by X-ray analysis. Both new DCI derivatives proved thermally stable compounds resisting decomposition over 270 °C. Optical properties were investigated by absorption and emission spectroscopy, which revealed blue-shifted CT-bands of **2** and **3** in comparison to **1**. However, the fluorescence quantum yields and Stokes shifts are larger. As the electrochemical data were not measurable, these were substituted by DFT calculations. The calculations showed larger HOMO-LUMO gaps for DCI analogues and also more positive/negative ground and excited state oxidation/reduction potentials. The differences in properties of DCP and DCI push-pull molecules also significantly affected their photoredox catalytic performance in cross-dehydrogenative coupling reaction in which the latter showed reduced capability.

We believe that this structure-property relationship study would serve as useful guide in designing new organic photoredox catalysts for visible light promoted reactions.

Experimental Section

General. Reagents and solvents were reagent-grade and were purchased from Penta, Aldrich, and TCI and used as received. The starting imidazole-4,5-dicarbonitrile, 2-methoxythiophene, and thiophen-2-ylboronic acid (**5**) were commercially available. Compounds **1**²⁵ and **4**^{32,37,38} were prepared according to literature. All cross-coupling reactions were carried out in flame-dried flasks under argon atmosphere. Thin layer chromatography (TLC) was conducted on aluminum sheets coated with silica gel 60 F₂₅₄ with visualization by a UV lamp (254 or 360 nm). Column chromatography was carried out with silica gel 60 (particle size 0.040-0.063 mm, 230-400 mesh) and commercially available solvents. All ¹H and ¹³C NMR spectra were recorded on a Bruker AVANCE II/III 400/500 spectrometer (400/500 MHz or 100/25 MHz, respectively). Chemical shifts in ¹H and ¹³C NMR spectra are reported in ppm relative to the signal of Me₄Si (0.00 ppm). The residual solvent signal

in the ^1H and ^{13}C NMR spectra was used as an internal reference (CDCl_3 7.25 and 77.23 ppm). Apparent resonance multiplicities are described as s (singlet), d (doublet) and m (multiplet). ^1H NMR signals of thiophene moieties were denoted as Th. The coupling constants J are reported in Hertz (Hz). High-resolution MALDI mass spectroscopy data were collected on LTQ Orbitrap XL. IR spectra were recorded on a Perkin-Elmer FTIR Spectrum BX spectrometer. Mass spectra were measured on a GC-MS configuration comprised of an Agilent Technologies 6890N gas chromatograph equipped with a 5973 Network MS detector (EI 70 eV, mass range 33–550Da). UV-Vis spectra were recorded on a Hewlett-Packard 8453 and UV/Vis Perkin-Elmer Lambda 35 spectrophotometers in CH_2Cl_2 . The fluorescence emission spectra were measured on a PTI Quantmaster 40 steady state spectrofluorimeter. Thermal properties of target molecules were measured by differential scanning calorimetry DSC on Mettler-Toledo STARe System DSC 2/700 with ceramic sensor FRS 6 and cooling system HUBERT TC100-MT RC 23 in open aluminum crucibles under N_2 atmosphere. DSC curves were recorded with a scanning rate of $3\text{ }^\circ\text{C}/\text{min}$ within a range of 25 to $500\text{ }^\circ\text{C}$.

General method for Suzuki-Miyaura cross-coupling reactions (2 and 3). 2-Bromo-1-methyl-1*H*-imidazole-4,5-dicarbonitrile **4** (211 mg; 1.0 mmol) and **5** (140 mg; 1.1 mmol) or **6** (264 mg; 1.1 mmol) were dissolved in the mixture of THF/ H_2O (50 mL; 4:1). Argon was bubbled through the solution for 10 min, whereupon $[\text{Pd}_2(\text{dba})_3]$ (46 mg; 0.05 mmol; 5 mol%), SPhos (20.5 mg; 0.05 mmol; 5 mol%), and Cs_2CO_3 (358 mg; 1.1 mmol) were added and the reaction mixture was stirred at $65\text{ }^\circ\text{C}$ for the indicated reaction time. The reaction mixture was diluted with water (40 mL) and extracted with CH_2Cl_2 ($3 \times 40\text{ mL}$). The combined organic extracts were dried (Na_2SO_4) and the solvents were evaporated *in vacuo*. The crude product was purified by flash chromatography (SiO_2 ; CH_2Cl_2) and subsequent crystallization from 1,2-dichloroethane/hexane.

1-Methyl-2-(thiophen-2-yl)-1*H*-imidazole-4,5-dicarbonitrile (2). The title compound was synthesized from **4** and **5** according to the general method (6 h reaction time). Yield 128 mg (60%), colorless solid. mp $149\text{ }^\circ\text{C}$; R_f 0.51 (SiO_2 ; CH_2Cl_2); IR (ATR): λ_{max} 3103, 2232 (CN), 1359, 1324, 1224 cm^{-1} ; ^1H NMR (400 MHz, CDCl_3): δ_{H} 3.99 (3H, s, NCH_3), 7.21 (1H, dd, J 3.8 and 5.1 Hz, Th), 7.57 (1H, dd, J 1.1 and 3.8 Hz, Th), 7.60 ppm (1H, dd, J 1.1 and 5.1 Hz, Th); ^{13}C -NMR (125 MHz, CDCl_3): δ_{C} 34.7, 108.3, 111.5, 113.9, 122.3, 128.3, 128.8, 129.5, 130.4, 147.1 ppm. HR-FT-MALDI-MS (DHB) m/z : calcd. for $\text{C}_{10}\text{H}_7\text{N}_4\text{S}^+$ 215.03859 ($[\text{M}+\text{H}]^+$); found 215.03879.

2-(5-Methoxythiophen-2-yl)-1-methyl-1*H*-imidazole-4,5-dicarbonitrile (3). The title compound was synthesized from **4** and **6** according to the general method (72 h reaction time). Yield 61 mg (25%), colorless solid. mp $156\text{ }^\circ\text{C}$; R_f 0.31 (SiO_2 ; CH_2Cl_2); IR (ATR): λ_{max} 3109, 2232 (CN), 1356, 1326, 1253, 1218, 1073, 995 cm^{-1} ; ^1H NMR (500 MHz, CDCl_3): δ_{H} 3.94 (3H, s, OCH_3), 3.97 (3H, s, NCH_3), 6.28 (1H, d, J 4.0 Hz, Th), 7.21 ppm (1H, d, J 4.0 Hz, Th); ^{13}C -NMR (125 MHz, CDCl_3): δ_{C} 34.7, 60.8, 105.5; 108.7, 111.8, 113.6, 115.1, 122.3, 128.4, 147.4, 170.9 ppm. HR-FT-MALDI-MS (DHB) m/z : calcd. for $\text{C}_{11}\text{H}_9\text{N}_4\text{OS}^+$ 245.04916 ($[\text{M}+\text{H}]^+$); found 245.04913.

2-(5-Methoxythiophen-2-yl)-4,4,5,5-tetramethyl-1,3,2-dioxaborolane (6). A solution of 2-methoxythiophene (500 mg; 4.38 mmol) in dry THF (20 mL) was treated with *n*BuLi (3.1 mL; 5.04 mmol; 1.6 M sol. in hexane) at $-78\text{ }^\circ\text{C}$ under argon for 1 h. 2-Isopropoxy-4,4,5,5-tetramethyl-1,3,2-dioxaborolane (1.03 mL; 5.04 mmol; *i*PrOBpin) was added, the reaction mixture was allowed to reach $25\text{ }^\circ\text{C}$, and was stirred for 1 h. Saturated aqueous solution of NH_4Cl (10 mL) was added and the product was extracted with Et_2O ($3 \times 10\text{ mL}$). The combined organic extracts were dried (Na_2SO_4) and the solvents were evaporated *in vacuo* to afford **6**, which was used without further purification. Yield 936 mg (89%), yellow solid. mp $36\text{--}42\text{ }^\circ\text{C}$; ^1H NMR (500 MHz, CDCl_3): δ_{H} 1.31 (12H, s, 4 \times CH_3), 3.90 (3H, s, OCH_3), 6.29 (1H, d, J 4.0 Hz, Th), 7.32 ppm (1H, d, J 4.0 Hz, Th) ppm; ^{13}C -NMR (125 MHz, CDCl_3): δ_{C} 24.9, 60.6, 84.0, 106.3, 136.7, 173.0 ppm. EI-MS (70 eV) m/z (rel. int.): 240 (100, M^+), 225 (20), 197 (30), 180 (50), 167 (15), 155 (30), 140 (50), 125 (15), 97 (10), 83 (8). Spectral data were in accordance with the literature.⁴⁸

X-ray crystallographic data for 3. The X-ray data for colorless crystal of **3** were obtained at 150 K using Oxford Cryostream low-temperature device on a Nonius KappaCCD diffractometer with Mo/K α radiation (λ 0.71073 Å), a graphite monochromator, and the ϕ and χ scan mode. Data reductions were performed with DENZO-SMN.⁴⁹ The absorption was corrected by integration methods.⁵⁰ Structures were solved by direct methods (Sir92)⁵¹ and refined by full matrix least-square based on F^2 (SHELXL97).⁵²

Hydrogen atoms were mostly localized on a difference Fourier map but to ensure uniformity of treatment of crystal, all hydrogens were recalculated into idealized positions (riding model) and assigned temperature factors $H_{iso}(H) = 1.2 U_{eq}$ (pivot atom) or of $1.5U_{eq}$ (methyl). H atoms in methyl moieties and hydrogen atoms in aromatic ring were placed with C-H distances of 0.96 and 0.93 Å.

$R_{int} = \sum |F_o^2 - F_{o,mean}^2| / \sum F_o^2$, $GOF = [\sum (w(F_o^2 - F_c^2)^2) / (N_{diffs} - N_{params})]^{1/2}$ for all data, $R(F) = \sum | |F_o| - |F_c| | / \sum |F_o|$ for observed data, $wR(F^2) = [\sum (w(F_o^2 - F_c^2)^2) / (\sum w(F_o^2)^2)]^{1/2}$ for all data.

Relevant crystallographic data and structural refinement parameters for **3**: C₁₁H₈N₄OS, M = 244.27, triclinic, $P-1$, $a = 6.7170$ (2), $b = 9.2990$ (4), $c = 9.7339$ (5) Å, $\alpha = 87.081$ (3), $\beta = 78.441$ (2), $\gamma = 80.481$ (3) °, $Z = 2$, $V = 587.36$ (4) Å³, $D_c = 1.381$ g.cm⁻³, $\mu = 0.264$ mm⁻¹, $T_{min}/T_{max} = 0.940/0.974$; $-8 \leq h \leq 8$, $-12 \leq k \leq 12$, $-12 \leq l \leq 12$; 12492 reflections measured ($\theta_{max} = 27.49$ °), 2664 independent ($R_{int} = 0.032$), 2318 with $I > 2\sigma(I)$, 154 parameters, $S = 1.087$, $R1(obs. data) = 0.0452$, $wR2(all data) = 0.115$; max., min. residual electron density = 1.32, -0.445 eÅ⁻³.

Crystallographic data for structural analysis have been deposited with the Cambridge Crystallographic Data Centre, CCDC no. 1533813 for **3**. Copies of this information may be obtained free of charge from The Director, CCDC, 12 Union Road, Cambridge CB2 1EY, UK (fax: +44-1223-336033; e-mail: deposit@ccdc.cam.ac.uk or www: <http://www.ccdc.cam.ac.uk>).

Acknowledgements

We thank Z. Růžičková for carrying out X-ray diffraction experiment, refinement, and the obtained XRD data analysis of **3**; M. Klikar for measuring the DSC analyses; N. Almonasy for recording the emission spectra; O. Pytela for DFT calculations; and Z. Jiang for carrying out the CDC reactions.

Supplementary Material

¹H and ¹³C NMR, HR-MALDI-MS spectra, and DSC curves of **2**, **3**, and **6**.

References

- Romero, N. A.; Nicewicz, D. A. *Chem. Rev.* **2016**, *116*, 10075-10166.
<http://dx.doi.org/10.1021/acs.chemrev.6b00057>
- Narayanam, J. M. R.; Stephenson, C. R. *J Chem. Soc. Rev.* **2011**, *40*, 102-113.
<http://dx.doi.org/10.1039/b913880n>
- Tucker, J. W.; Zhang, Y.; Jamison, T. F.; Stephenson, C. R. *J. Angew. Chem. Int. Ed.* **2012**, *51*, 4144-4147.
<http://dx.doi.org/10.1002/anie.201200961>
- Tucker, J. W.; Stephenson, C. R. *J. Org. Chem.* **2012**, *77*, 1617-1622.

- <http://dx.doi.org/10.1021/jo202538x>
5. Xuan, J.; Xiao, W.-J. *Angew. Chem. Int. Ed.* **2012**, *51*, 6828-6838.
<http://dx.doi.org/10.1002/anie.201200223>
 6. Special Issue on "Photoredox Catalysis in Organic Chemistry", Stephenson, C.; Yoon, T. (Eds.). *Acc. Chem. Res.* **2016**, *49*, 2059-2060.
<http://dx.doi.org/10.1021/acs.accounts.6b00502>
 7. Yoon, T. P.; Ischay, M. A.; Du, J. *Nat. Chem.* **2010**, *2*, 527-532.
<http://dx.doi.org/10.1038/nchem.687>
 8. Protti, S.; Fagnoni, M. *Photochem. Photobiol. Sci.* **2009**, *8*, 1499-1516.
<http://dx.doi.org/10.1039/B909128A>
 9. Ravelli, D.; Dondi, D.; Fagnoni, M.; Albini, A. *Chem. Soc. Rev.* **2009**, *38*, 1999-2011.
<http://dx.doi.org/10.1039/B714786B>
 10. Fagnoni, M.; Dondi, D.; Ravelli, D.; Albini, A. *Chem. Rev.* **2007**, *107*, 2725-2756.
<http://dx.doi.org/10.1021/cr068352x>
 11. Prier, C. K.; Rankic, D. A.; MacMillan, D. W. C. *Chem. Rev.* **2013**, *113*, 5322-5363.
<http://dx.doi.org/10.1021/cr300503r>
 12. Zhang, X.; MacMillan, D. W. C. *J. Am. Chem. Soc.* **2016**, *138*, 13862-13865.
<http://dx.doi.org/10.1021/jacs.6b09533>
 13. Nicewicz, D. A.; MacMillan, D. W. C. *Science* **2008**, *322*, 77-80.
<http://dx.doi.org/10.1126/science.1161976>
 14. Nagib, D. A.; MacMillan, D. W. C. *Nature* **2011**, *480*, 224-228.
<http://dx.doi.org/10.1038/nature10647>
 15. McNally, A.; Prier, C. K.; MacMillan, D. W. C. *Science* **2011**, *334*, 1114-1117.
<http://dx.doi.org/10.1126/science.1213920>
 16. Pirnot, M. T.; Rankic, D. A.; Martin, MacMillan, D. W. C. *Science* **2013**, *339*, 1593-1596.
<http://dx.doi.org/10.1126/science.1232993>
 17. Zuo, Z.; Cong, H.; Li, W.; Choi, J.; Fu, G. C.; MacMillan, D. W. C. *J. Am. Chem. Soc.* **2016**, *138*, 1832-1835.
<http://dx.doi.org/10.1021/jacs.5b13211>
 18. Guo, W.; Lu, L.-Q.; Wang, Y.; Wang, Y.-N.; Chen, J.-R.; Xiao, W.-J. *Angew. Chem. Int. Ed.* **2015**, *54*, 2265-2269.
<http://dx.doi.org/10.1002/anie.201408837>
 19. Prasad, D.; König, B. *Chem. Commun.* **2014**, *50*, 6688-6699.
<http://dx.doi.org/10.1039/C4CC00751D>
 20. Majek, M.; Filace, F.; von Wangelin, A. J. *Chem. Eur. J.* **2015**, *21*, 4518-4522.
<http://dx.doi.org/10.1002/chem.201406461>
 21. Liu, H.; Feng, W.; Kee, C. W.; Zhao, Y.; Leow, D.; Pan, Y.; Tan, C.-H. *Green Chem.* **2010**, *12*, 953-956.
<http://dx.doi.org/10.1039/B924609F>
 22. Bureš, F. *RSC Adv.* **2014**, *4*, 58826-58851.
<http://dx.doi.org/10.1039/C4RA11264D>
 23. Klikar, M.; Solanke, P.; Tydlitát, J.; Bureš, F. *Chem. Rec.* **2016**, *16*, 1886-1905.
<http://dx.doi.org/10.1002/tcr.201600032>
 24. Bureš, F.; Čermáková, H.; Kulhánek, J.; Ludwig, M.; Kuzník, W.; Kityk, I. V.; Mikysek, T.; Růžička, A. *Eur. J. Org. Chem.* **2012**, 529-538.
<http://dx.doi.org/10.1002/ejoc.201101226>

25. Zhao, Y.; Zhang, C.; Chin, K. F.; Pytela, O.; Wei, G.; Liu, H.; Bureš, F.; Jiang, Z. *RSC Adv.* **2014**, *4*, 30062-30067.
<http://dx.doi.org/10.1039/C4RA05525J>
26. Condie, A. G.; Gonzáles-Gómez, J. C.; Stephenson, C. R. J. *J. Am. Chem. Soc.* **2010**, *132*, 1464-1465.
<http://dx.doi.org/10.1021/ja909145y>
27. Liu, X.; Ye, X.; Bureš, F.; Liu, H.; Jiang, Z. *Angew. Chem. Int. Ed.* **2015**, *54*, 11443-11447.
<http://dx.doi.org/10.1002/anie.201505193>
28. Zhang, C.; Li, S.; Bureš, F.; Lee, R.; Ye, X.; Jiang, Z. *ACS Catal.* **2016**, *6*, 6853-6860.
<http://dx.doi.org/10.1021/acscatal.6b01969>
29. Wei, G.; Zhang, C.; Bureš, F.; Ye, X.; Tan, C.-H.; Jiang, Z. *ACS Catal.* **2016**, *6*, 3708-3712.
<http://dx.doi.org/10.1021/acscatal.6b00846>
30. Bureš, F. *Chem Listy* **2013**, *107*, 834-842.
31. Kulhánek, J.; Bureš, F. *Beilstein J. Org. Chem.* **2012**, *8*, 25-49.
<http://dx.doi.org/10.3762/bjoc.8.4>
32. Kulhánek, J.; Bureš, F.; Pytela, O.; Mikysek, T.; Ludvík, J.; Růžička, A. *Dyes Pigm.* **2010**, *85*, 57-65.
<http://dx.doi.org/10.1016/j.dyepig.2009.10.004>
33. Nepraš, M.; Almonasy, N.; Bureš, F.; Kulhánek, J.; Dvořák, M.; Michl, M. *Dyes Pigm.* **2011**, *91*, 466-473.
<http://dx.doi.org/10.1016/j.dyepig.2011.03.025>
34. Kulhánek, J.; Bureš, F.; Wojciechowski, A.; Makowska-Janusik, M.; Gondek, E.; Kityk, I. V. *J. Phys. Chem. A* **2010**, *114*, 9440-9446.
<http://dx.doi.org/10.1021/jp1047634>
35. Plaquet, A.; Champagne, B.; Kuhlank, J.; Bureš, F.; Bogdan, E.; Castet, F.; Ducasse, L.; Rodriguez, V. *ChemPhysChem* **2011**, *12*, 3245-3252.
<http://dx.doi.org/10.1002/cphc.201100299>
36. Kulhánek, J.; Bureš, F.; Pytela, O.; Mikysek, T.; Ludvík, J. *Chem. Asian J.* **2011**, *6*, 1604-1612.
<http://dx.doi.org/10.1002/asia.201100097>
37. Apen, P. G.; Rasmussen, P. G. *Heterocycles* **1989**, *29*, 1325-1329.
<http://dx.doi.org/10.3987/COM-89-4980>
38. O'Connell, J. F.; Parquette, J.; Yelle, W. E.; Wang, W.; Rapoport, H. *Synthesis* **1988**, 767-771.
<http://dx.doi.org/10.1055/s-1988-27702>
39. Achelle, S.; Ramondenc, Y.; Marsais, F.; Plé, N. *Eur. J. Org. Chem.* **2008**, 3129-3140.
<http://dx.doi.org/10.1002/ejoc.200800139>
40. Bird, C. W. *Tetrahedron* **1986**, *42*, 89-92.
<http://dx.doi.org/10.1016/S0040-4020>
41. Bird, C. W. *Tetrahedron* **1985**, *41*, 1409-1414.
<http://dx.doi.org/10.1016/S0040-4020>
42. Kotelevskii, S. I.; Prezhdo, O. V. *Tetrahedron* **2001**, *57*, 5715-5729.
<http://dx.doi.org/10.1016/S0040-4020>
43. Krygowski, T. M.; Szatylowicz, H.; Stasyuk, O. A.; Dominikowska, J.; Palusiak, M. *Chem. Rev.* **2014**, *114*, 6383-6422.
<http://dx.doi.org/10.1021/cr400252h>
44. Solanke, P.; Bureš, F.; Pytela, O.; Klikar, M.; Mikysek, T.; Mager, L.; Barsella, A.; Růžičková, Z. *Eur. J. Org. Chem.* **2015**, *24*, 5339-5349.
<http://dx.doi.org/10.1002/ejoc.201500525>

45. Liu, X.; Xu, Z.; Cole, J. M. *J. Phys. Chem. C* **2013**, *117*, 16584-16905.
<http://dx.doi.org/10.1021/jp404170w>
46. Gaussian 09, Revision D.01, M. J. Frisch, G. W. Trucks, H. B. Schlegel, G. E. Scuseria, M. A. Robb, J. R. Cheeseman, G. Scalmani, V. Barone, B. Mennucci, G. A. Petersson, H. Nakatsuji, M. Caricato, X. Li, H. P. Hratchian, A. F. Izmaylov, J. Bloino, G. Zheng, J. L. Sonnenberg, M. Hada, M. Ehara, K. Toyota, R. Fukuda, J. Hasegawa, M. Ishida, T. Nakajima, Y. Honda, O. Kitao, H. Nakai, T. Vreven, J. A. Montgomery, Jr., J. E. Peralta, F. Ogliaro, M. Bearpark, J. J. Heyd, E. Brothers, K. N. Kudin, V. N. Staroverov, T. Keith, R. Kobayashi, J. Normand, K. Raghavachari, A. Rendell, J. C. Burant, S. S. Iyengar, J. Tomasi, M. Cossi, N. Rega, J. M. Millam, M. Klene, J. E. Knox, J. B. Cross, V. Bakken, C. Adamo, J. Jaramillo, R. Gomperts, R. E. Stratmann, O. Yazyev, A. J. Austin, R. Cammi, C. Pomelli, J. W. Ochterski, R. L. Martin, K. Morokuma, V. G. Zakrzewski, G. A. Voth, P. Salvador, J. J. Dannenberg, S. Dapprich, A. D. Daniels, O. Farkas, J. B. Foresman, J. V. Ortiz, J. Cioslowski, D. J. Fox, Gaussian, Inc., Wallingford CT, **2013**.
47. Isse, A. A.; Gennaro, A. *J. Phys. Chem. B* **2010**, *114*, 7894-7899.
<http://dx.doi.org/10.1021/jp100402x>
48. Fukurawa, T.; Tobisu, M.; Chatani, N. *J. Am. Chem. Soc.* **2015**, *137*, 12211-12214.
<http://dx.doi.org/10.1021/jacs.5b07677>
49. Otwinowski, Z.; Minor, W. *Methods Enzymol.* **1997**, *276*, 307-326.
<http://dx.doi.org/10.1016/S0076-6879>
50. Coppens, P. in Ahmed, F. R.; Hall, S.R.; Huber, C. P., Eds., *Crystallographic Computing*, **1970**, 255-270, Copenhagen, Munksgaard.
51. Altomare, A.; Casciarano, G.; Giacovazzo, C.; Guagliardi, A. *J. Appl. Crystallogr.* **1994**, *27*, 1045-1050.
<https://dx.doi.org/10.1107/S002188989400422X>
52. Sheldrick, G. M. *Acta Crystallogr., Sect. A: Found. Adv.* **2015**, *A71*, 3-8.
<https://dx.doi.org/10.1107/S2053273314026370>